Lifetime measurements of the low-lying excited states of 208Po

Kocheva, D.; Yaneva, A.; Kalaydjieva, D.; Rainovski, G.; Jolie, J.; Pietralla, N.; Beckers, M.; Blazhev, A.; Bussmann, L.; Cappellazzo, M.; Dewald, A.; Diel, F.; Djongolov, M.; Dunkel, F.; Esmaylzadeh, A.; Falk, B.; Fransen, C.; Garbe, J.; Gerhard, L.; Gerst, R.-B.; Gladnishki, K. A.; Goldkuhle, A.; Hackenberg, G.; Henrich, C.; Homm, I.; Ide, K.; Karayonchev, V.; Kern, R.; Kleemann, J.; Knafla, L.; Kornwebel, L.; Kröll, Th.; Ley, M.; Muller-Gatermann, C.; Scheck, M.; Schmidt, T.; Spagnoletti, P.; Stoyanova, M.; Werner, M.

Published in:
Journal of Physics: Conference Series

DOI:
10.1088/1742-6596/1555/1/012020

Published: 01/05/2020

Document Version
Publisher's PDF, also known as Version of record

Lifetime measurements of the low-lying excited states of ^{208}Po

Journal of Physics: Conference Series **1555** (2020) 012020 doi:10.1088/1742-6596/1555/1/012020

Lifetime measurements of the low-lying excited states of ^{208}Po

D. Kocheva[1], A. Yaneva[1], D. Kalaydjieva[1], G. Rainovski[1], J. Jolie[2], N. Pietralla[3], M. Beckers[2], A. Blazhev[2], L. Bussmann[2], M. Cappellazzo[2], A. Dewald[2], F. Diel[2], M. Djongolov[1], F. Dunkel[2], A. Esmaylzadeh[2], B. Falk[2], C. Fransen[2], J. Garbe[2], L. Gerhard[2], R.-B. Gerst[2], K. A. Gladnishki[1], A. Goldkuhle[2], G. Hackenberg[2], C. Henrich[3], I. Homm[3], K. Ide[3], V. Karayonchev[2], R. Kern[3], J. Kleeman[3], L. Knafla[2], L. Kornwebel[2], Th. Kröll[3], M. Ley[2], C. Müller-Gatermann[2], M. Scheck[4], T. Schmidt[2], P. Spagnoletti[4], M. Stoyanova[1], V. Werner[3]

[1] Faculty of Physics, St. Kliment Ohridski University of Sofia, 1164 Sofia, Bulgaria
[2] Institut für Kernphysik, Universität zu Köln, 50937 Cologne, Germany
[3] Institut für Kernphysik, Technische Universität Darmstadt, 64289 Darmstadt, Germany
[4] University of the West of Scotland, PA1 2BE Paisley, UK and SUPA, Glasgow G12 8QQ, UK

E-mail: dkocheva@phys.uni-sofia.bg

Abstract. In this study we present the preliminary results about the lifetimes of the 2_2^+, 4_1^+ states of ^{208}Po and the upper limit of the lifetime of the 2_1^+ state. For measuring the lifetimes of the 2_1^+ and 4_1^+ states the Recoil Distance Doppler Shift (RDDS) method and for the lifetime of the 2_2^+ state the Doppler Shift Attenuation method (DSAM) were used. The resulting absolute transition strength $B(M1; 2_2^+ \rightarrow 2_1^+) \geq 0.122(20)\ \mu_N^2$ reveals the predominant isovector nature of the 2_2^+ state of ^{208}Po.

1. Introduction

The properties of open-shell nuclei in the immediate vicinity of doubly-magic cores are of particular importance because such nuclei can often be understood well within the framework of the shell model [1] and at the same time their valence particles can induce the onset of collective behavior [2]. The nucleus ^{208}Po has two valence protons and two neutron holes with respect to the doubly-magic core ^{208}Pb. The simplest possible description of the low-lying states of this nucleus can be pursued in the framework of an empirical single-j shell model approximation since the effective nuclear interaction can be deduced from the energy spectra of the neighbouring nuclei. In this approach ^{206}Pb corresponds to two neutron holes while ^{210}Po corresponds to two protons with respect to the ^{208}Pb core. In our previous studies we measured the lifetimes of the first three 2^+ excited states of the nucleus ^{212}Po which is situated at the opposite side of ^{208}Po with respect to the neutron number around the ^{208}Pb core. The experimental results indicate that the 2_2^+ state of ^{212}Po is an isovector state [3] and the derived $B(E2; 2_1^+ \rightarrow 0_1^+)$ value indicates a low collectivity in the structure of the first excited state of ^{212}Po [4]. In order to study these properties in the case of the nucleus ^{208}Po experimental information on the

absolute transition strenghts of its low-lying 2^+ excited states is needed. This has motivated us to perform two experiments for measuring the lifetimes of the 2_1^+ and 2_2^+ excited states of ^{208}Po. Both experiments were performed at the FN Tandem facility at the University of Cologne, Germany.

2. Lifetime measurement of the 2_2^+ state of ^{208}Po

2.1. Experimental set-up

For measuring the lifetime of the 2_2^+ state of ^{208}Po by means of DSAM (cf. Ref. [5] and references therein) the ^{204}Pb(^{12}C,^{8}Be)^{208}Po transfer reaction was used. The beam energy was choosen to be 62 MeV. The target was a self-supporting 23 mg/cm^2 thick Pb foil enriched up to 99.94% in the isotope ^{204}Pb. The reaction was induced in the reaction chamber of the Cologne coincidence plunger device [6]. In order to detect the recoiling light reaction fragments an array of solar cells was mounted at backward angles covering an angular range between 116.8° and 167.2°. The solar cells were placed in the plunger chamber at a distance of about 15 mm between their centres and the target. ^{8}Be decays immediately after the reaction to two α-particles. In order to detect these α-particles but to stop other heavier fragments from additional transfer reactions an Al foil was placed between the target and the solar cells. The thickness of the foil was 80 μm. The γ rays from the decay of the excited states of ^{208}Po were registered by 11 HPGe detectors mounted outside the plunger chamber in two rings at distance of, on average, 12 cm from the target. Five detectors were positioned at backward angles (142° with respect to the beam axis) and the other six detectors were placed at forward angles (45° with respect to the beam axis). The set up also included 7 LaBr detectors for fast-timing measurements. The results from these measurements are presented in Ref. [7].

2.2. Data analysis and results

The data were sorted in coincidence mode of at least one solar cell and one HPGe detector (particle-γ) and when at least two HPGe detectors (γ-γ) were in coincidence. A partial level scheme of the states of ^{208}Po populated in the present experiment was constructed on the basis of the γ-γ coincidences. The level scheme is presented in Fig. 1 and is in agreement with the previously reported level schemes of ^{208}Po [8]. For the spin-parities of the observed states we adopted the values reported in the previous studies [8].

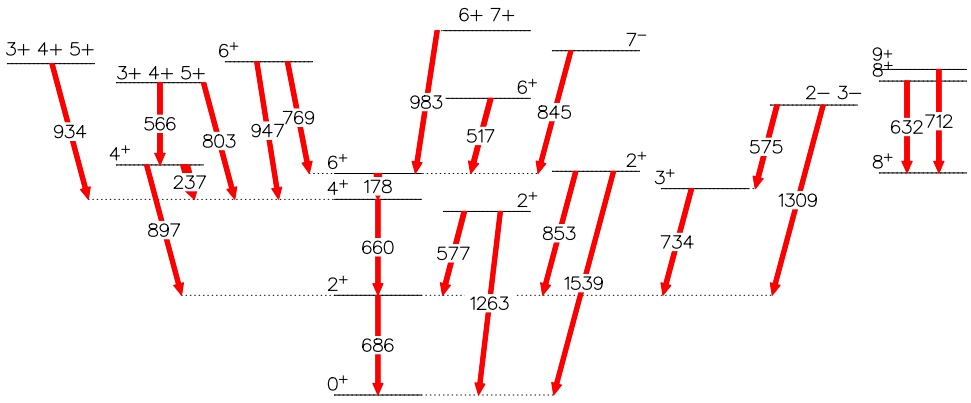

Figure 1. (Color online) Partial level scheme of ^{208}Po obtained in the present work

The particle-γ coincidence data were sorted in two matrices depending on the position of the HPGe detectors. A projection of the particle-γ matrix obtained with γ-ray detection at 45° is shown in Fig. 2(a). The γ rays in coincidence with the group of particles labeled as "^{208}Po" in

Fig. 2(a) are shown in Fig. 2(b). This spectrum is dominated by the 686-keV and the 660-keV lines which are the γ-ray transitions depopulating the first two yrast states of ^{208}Po [8]. The 576-keV and 1263-keV γ-ray lines show Doppler shapes which allow us to extract the lifetime of the 2_2^+ state of ^{208}Po (cf. Fig 1).

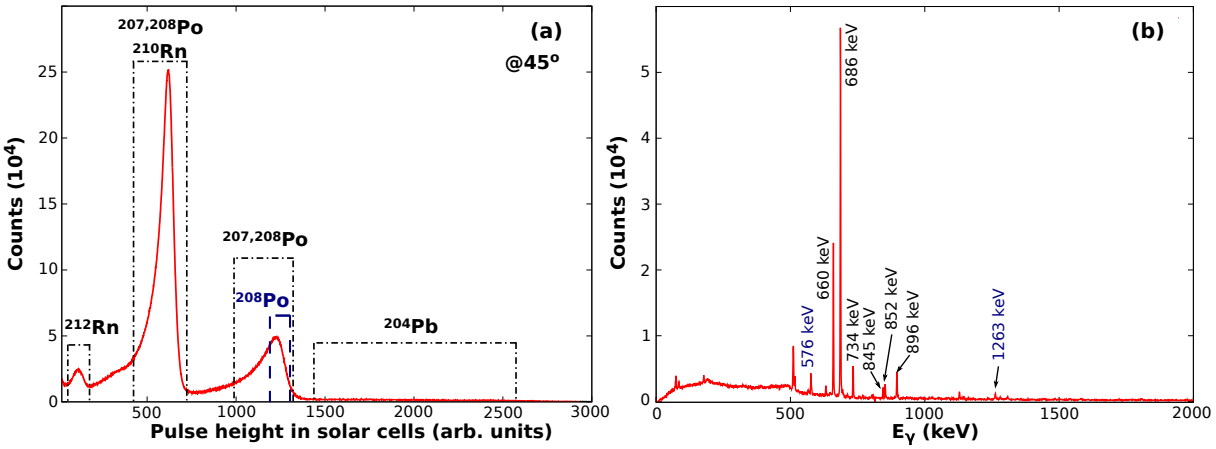

Figure 2. (Color online) (a) The projection of the particle-γ matrix obtained by coincidence detection of charged particles in the solar-cell array and γ rays at $\Theta_\gamma = 45°$ polar angle. The dashed boxes represent parts of the particle spectrum found to be in coincidence with γ rays from the indicated nuclei. (b) The γ-ray spectrum in coincidence with the group of particles indicated as "^{208}Po" in panel (a).

The line-shape analysis was performed with the integrated software package APCAD (Analysis Program for Continuous Angle DSAM) [9]. In APCAD, the slowing down process is simulated by GEANT4 [10]. The electronic stopping powers were taken from the Northcliffe and Schilling tables [11] with corrections for the atomic structure of the medium, as discussed in Ref. [12]. The angular straggling due to nuclear collisions is modelled discretely by means of Monte Carlo simulation while the corresponding energy loss is considered to emerge as a result from a continuous process for which the nuclear stopping powers were taken from SRIM2013 [13] and reduced by 30% [14]. The analysis accounts for the response of the HPGe detectors, for the experimental geometry, and for the restrictions on the reaction kinematics imposed by the solar-cell array.

The lifetime of the second excited 2^+ state of ^{208}Po was obtained from the line shapes of the 576-keV ($2_2^+ \rightarrow 2_1^+$) and 1263-keV ($2_2^+ \rightarrow 0_1^+$) transitions. Special care was taken into account for the impact of the 575-keV ($2^-, 3^- \rightarrow 3_1^+$) transition which contributes extra counts to the intensity of the 576-keV ($2_2^+ \rightarrow 2_1^+$) line (cf. Fig 1). In order to determine the contribution of the counts coming from the 575-keV transition we used the intensity of the 1309-keV ($2^-, 3^- \rightarrow 2_1^+$) transition which does not exhibit a Doppler shape in the present data. The branching ratio [8] and the efficiency calibration were taken into account as well. The line-shape fits of the 576-keV ($2_2^+ \rightarrow 2_1^+$) and 1263-keV ($2_2^+ \rightarrow 0_1^+$) transitions are shown in Fig. 3 (a) and Fig. 3 (b), respectively. Here an unidentified stopped contaminant with $E_\gamma = 1258$ keV is fitted simultaneously with the 1263-keV line. Under this assumption, the value of the lifetime of the 2_2^+ state is extracted to be 1.12(18) ps. The lifetime together with the available spectroscopic information and the resulting transition strengths are summarized in Table 1.

3. Lifetime measurements of the 2_1^+ and 4_1^+ states of ^{208}Po

3.1. Experimental set-up

The lifetime of the 2_1^+ state of ^{208}Po was measured by utilizing the RDDS method [5, 15]. The same reaction was used as for the DSAM experiment. The target consisted of a 0.6 mg/cm^2 thin

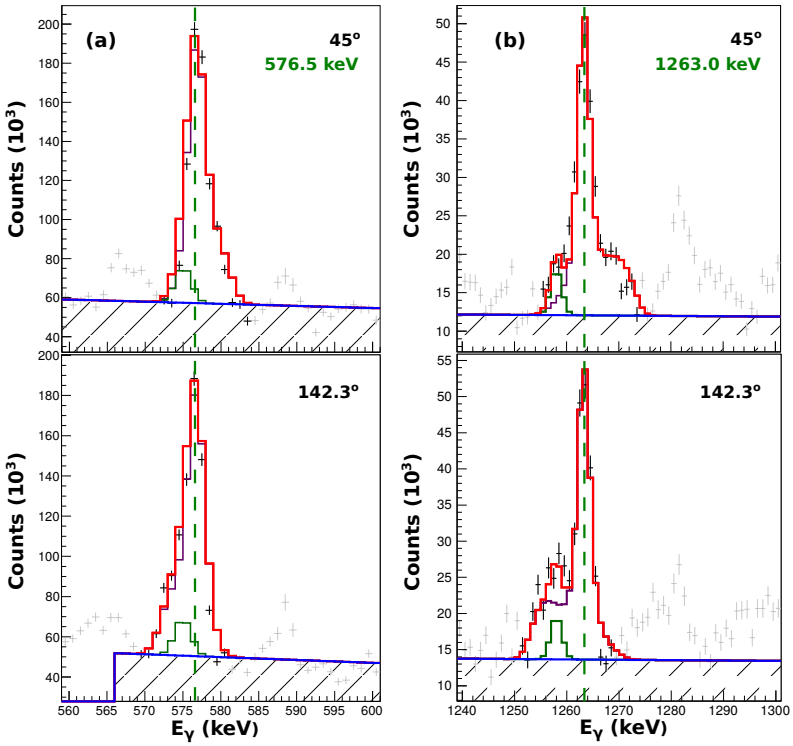

Figure 3. (Color online) The line-shape fits of the 576-keV ($2_2^+ \rightarrow 2_1^+$) (a) and the 1263-keV ($2_2^+ \rightarrow 0_1^+$) (b) transitions obtained with the program APCAD. The solid (red) line represents the total fit. The contribution of the counts stemming from the 575-keV ($2^-, 3^- \rightarrow 3_1^+$) transition is taken into account (green) (a). An unidentified stopped contaminant with $E_\gamma = 1258$ keV is fitted simultaneously (green) with the 1263-keV line (b).

Table 1. Properties of the 2_2^+ state of ^{208}Po and γ-ray transitions originating from its decay. Given are the excitation energy (E_{level}), the spin and parity quantum numbers of the initial level (J^π) and of the final levels (J^π_{final}), the energies (E_γ), the relative intensities (I_γ), the total electron conversion coefficient (α), and the multipole mixing ratio (δ) of the γ-rays transitions [8]. The lifetime of the state and the absolute transition strengths are from the present study, $B(E2)$ values are given in e^{2}fm^4 (1 W.u.= 73.21 e^{2}fm^4), and the $B(M1)$ values are given in μ_N^2.

E_{level} (keV)	J^π	J^π_{final}	E_γ (keV)	I_γ %	α	δ	τ (ps)	Transition strength $J^\pi \rightarrow J^\pi_{final}$
1263.0	2_2^+	0_1^+	1263.0	64(7)			1.12(18)	$B(E2) = 89(16)$
		2_1^+	576.5	100(11)	0.085(7)	≤ 0.48		$B(M1) \geq 0.122(20)$
								$B(E2) \leq 1210(200)$

layer of ^{204}Pb evaporated on a 1.5 mg/cm^2 thick Ta backing foil and was placed with the Ta foil facing the beam. The stopper was a self-supporting 5.8 mg/cm^2 thick Ta foil. The detector setup is the same to the one used for measuring the lifetime of the 2_2^+ state. The same Al foil between the target and the solar cells was placed at this experiment as well. Data were taken at seven plunger distances: 19(3)μm, 34(3)μm, 57(3)μm, 91(3)μm, 115(3)μm, 208(4)μm and 309(4)μm.

3.2. Data analysis and results

The particle-γ coincidence data were sorted in matrices depending on the positions of the HPGe detectors and the plunger distances. A projection on the particle axis of the particle-γ matrix

obtained with γ-ray detection at 142° at a plunger distance of 34 μm is shown in Fig. 4(a) as an example. Additional nuclei are populated at this experiment in comparison to the DSAM experiment due to reactions induced on the backing and/or on the stopper. The γ rays in coincidence with the group of particles labeled as "^{208}Po & ^{185}Re" in Fig. 4(a) are shown in Fig. 4(b). The 686- and 660-keV lines which are the γ-ray transitions depopulating the first two yrast states of ^{208}Po [8] are clearly visible. Moreover, it is also visible from Fig. 5 that both transitions have a well pronounced shifted component which evolves as a function of plunger distance and allows to determine the lifetimes of the 2_1^+ and 4_1^+ states of ^{208}Po. The spectra are normalized with respect to the total number of counts in the particle gate (cf. Fig. 4(a)) and, as a result, the total numbers of counts in the 686-keV and 660-keV transitions (the sum of the shifted and the unshifted components) remain constant for all distances.

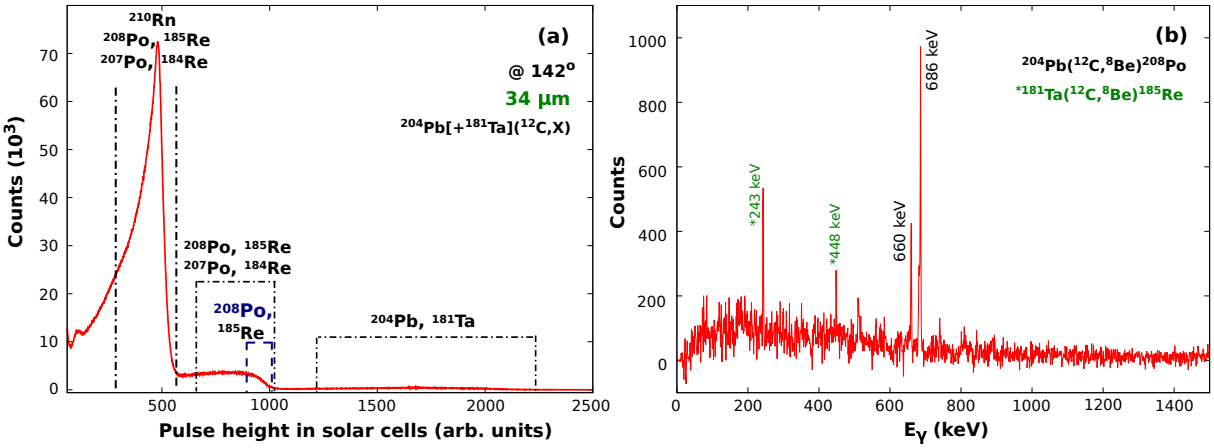

Figure 4. (Color online) (a) The projection of the particle-γ matrix obtained at plunger distance (D=34 μm) by coincident detection of charged particles in the solar-cell array and γ rays at a polar angle $\Theta_\gamma = 142°$. The marked ranges represent parts of the particle spectrum found to be in coincidence with the γ rays from the indicated nuclei. (b) The γ-ray spectrum in coincidence with the group of particles labeled as "^{208}Po & ^{185}Re" in panel (a).

The lifetime of the 4_1^+ state was determined using the Decay Curve Method where the measurement of the intensities of the shifted (I_{sh}) and unshifted (I_{un}) components as a function of the plunger distance gives the lifetime if the velocity of the recoiling nuclei is known [15]. The mean velocity $\langle v \rangle = 0.75(4)\%$c was experimentally determined from the centroids of the I_{sh}^{γ} and I_{un}^{γ} components. For extracting the lifetime of the 4_1^+ state the four longer distances in our data were used. In order to measure correctly the intensities of both components all transitions which feed directly the state of interest have to be taken into account. Fig. 1 shows that the 4_1^+ state has five direct feeders. Using the data from our DSAM experiment and the efficiency calibration we determined the relative population of the 4_1^+ state. The 6_1^+ state is long-lived and it decays only at rest [8] which means that the 178-keV transition contributes only to the stopped component of the 660-keV line. Hence, that extra contribution has to be accounted. In our analysis this was achieved by reducing the intensity of the unshifted component of the 660-keV line with intensity coming from the decay of the 6_1^+ state. The lifetimes of the other four feeders are not known and cannot be determined whether they are short- or long-lived. First we can assume that their lifetimes are sufficiently short so that they decay only in flight which results in $\tau(4_1^+)$ =157(30) ps. To investigate the influence of these feeders on the lifetime of the 4_1^+ state further, we have also considered the alternative limit that they are long-lived and decay exclusively at rest. Then an additional reduction of the intensity of the stopped component of 660-keV line has been done what results in $\tau(4_1^+)$ =133(24) ps. Then we can conclude that the

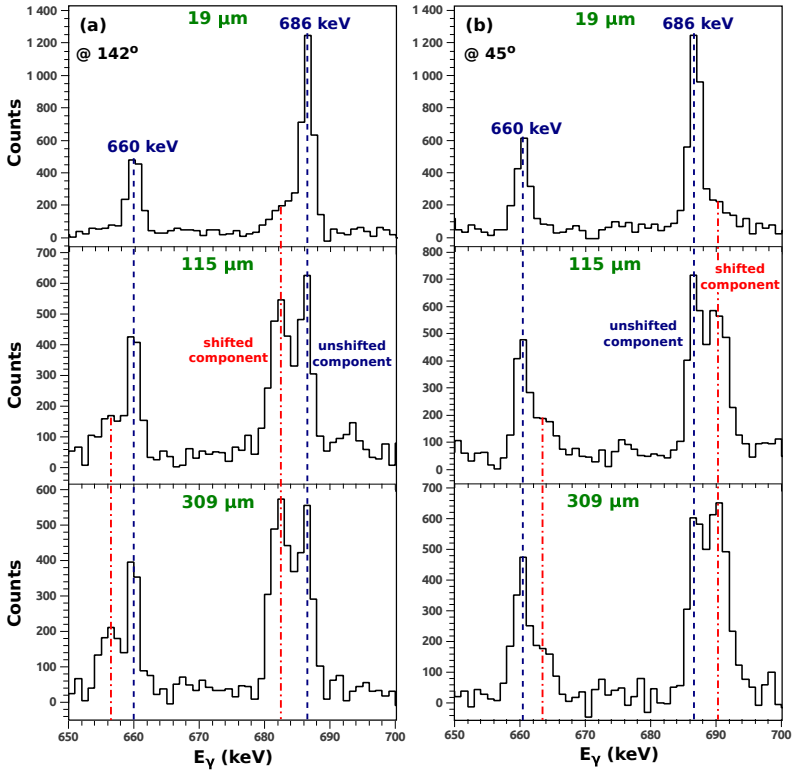

Figure 5. (Color online) Examples of the evolution of the intensities of the Doppler-shifted peaks of the 686-keV ($2_1^+ \rightarrow 0_1^+$) and 660-keV ($4_1^+ \rightarrow 2_1^+$) transitions observed at backward angles (a) and at forward angles (b) for three different target-to-stopper distances. The dot-dashed lines (red) represent the positions of the Doppler-shifted peak and the dashed lines (blue) represent the unshifted peak positions.

lifetime of the 4_1^+ state is expected to be 109 ps$< \tau(4_1^+) <$187 ps.

The RDDS data for 686-keV transition was analysed by utilizing the Differential Decay Curve Method (DDCM) [16, 17]. The standard application of DDCM requires the I_γ^{sh} and I_γ^{un} components (for each distance) to be measured from spectra in coincidence with Doppler-shifted components of transitions that feed directly the excited state of interest. Then the lifetime τ_i of the level of interest for the i-th target-to-stopper distance depends on I_{sh} and I_{un} in the simple way [16, 17]:

$$\tau_i(x) = \frac{I_{un}(x)}{\langle v \rangle \frac{d}{dx} I_{sh}(x)} \tag{1}$$

as here the derivative of the Doppler-shifted intensities as a function of the target-to-stopper distance, $\frac{d}{dx} I_{sh}$, is determined by a piecewise polynomial fit to the measured intensities I_{sh}. For the present experiment this would require analyzing particle-γ-γ data which is not possible at the acquired level of statistics. However, the particular feeding pattern of the 2_1^+ state of ^{208}Po allows this problem to be circumvented as described below. Analogous to the analysis of the 4_1^+ state we have estimated the intensities of transitions directly feeding the 2_1^+ state. The lifetime of the 2_2^+ state of ^{208}Po was measured in the present study to be short-lived, consequently, it contributes only to the fast feeding of the 2_1^+ state. The lifetime of the 2_3^+ state is assumed also to be very short-lived due to the 853-keV line shows Doppler shape in our DSAM data. The lifetimes of the 3_1^+, 4_2^+ and $2^-(3^-)$ states are not known and in order to simplify the discussion at this moment we assume that their lifetimes are short so that they decay only in flight. Under this assumption the only essential feeder to the 2_1^+ state remains the 660-keV transition which

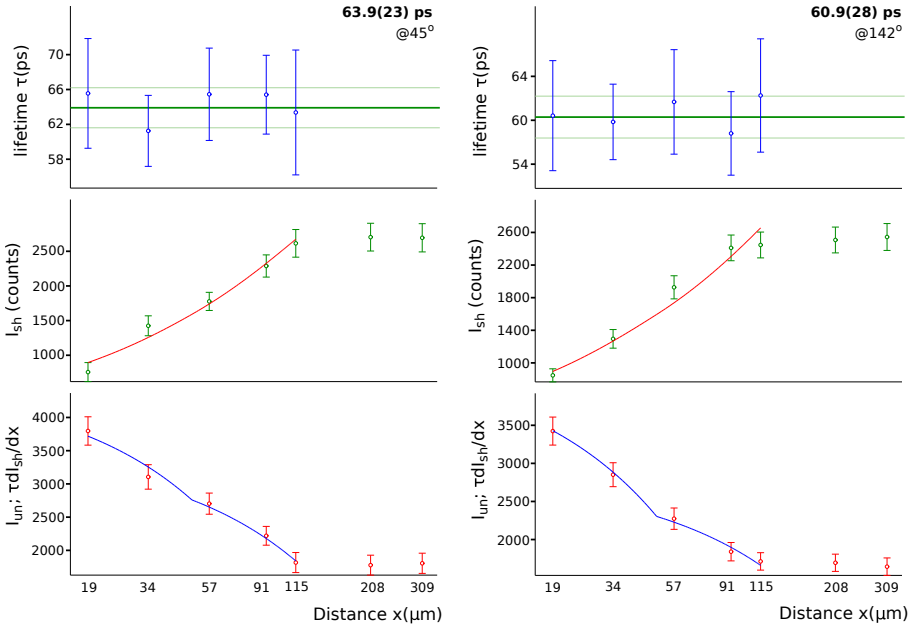

Figure 6. (Color online) The effective lifetime of the 2_1^+ state of ^{208}Po determined at forward (a) and backward angles (b). The middle panels show the shifted intensities at different distances. Continuous curves are fitted through the points to calculate the derivative. In the bottom panels, curves that represent the product between the time derivatives of the shifted intensities and the lifetime of the level are compared with the experimental unshifted intensities. Out of this comparison, the lifetimes corresponding to each distance in the region of sensitivity are extracted, as seen in the upper panel. The horizontal lines represent the weighted mean values.

depopulates the 4_1^+ state of ^{208}Po. The DDCM fits shown in Fig. 6 result in a weighted mean value for the effective lifetime of the 2_1^+ state of $\tau_{eff}(2_1^+)$ =62.4(21) ps. This value could be accepted as an upper limit of the lifetime of the 2_1^+ state of ^{208}Po.

4. Discussion

The structure of the first levels of ^{208}Po could be decribed as a superposition of the excitations in its neighbouring nuclei ^{206}Pb and ^{210}Po. The low energy of the 2_1^+ state (686 keV) indicates that the neutron part of its wave function is likely stronger than the proton one (see Fig. 7). In order to determine the wave function of the 2_1^+ state of ^{208}Po we have applied the approach of two-state mixing. The initial states here are the 2_1^+ states of ^{206}Pb and ^{210}Po and in our mixing calculations the excited states of these nuclei serve as pure proton and neutron excitations. The mixed $2_{I,II}^+$ states can be expressed as $|2_{I,II}^+\rangle = \alpha|\nu^{-2}\rangle \pm \beta|\pi^2\rangle$ where the "+" and the "-" signs are associated with the "I" and the "II" labels, respectively. By imposing the condition that the energy of the lower 2_I^+ mixed state coincides with the energy of the 2_1^+ state of ^{208}Po we have calculated that the effective proton-neutron residual interaction causing the mixing is V_{mix}=241 keV and the energy of the 2_{II}^+ mixed state is $E_{level}(2_{II}^+)$=1298 keV which is in good agreement with $E_{level}(2_2^+;^{208}\,\mathrm{Po})$=1263 keV. Under these assumptions the wave function of the 2_1^+ state of ^{208}Po is calculated to be:

$$|2_I^+\rangle = |2_1^+;^{208}\,\mathrm{Po}\rangle = 0.90|\nu^{-2}\rangle + 0.44|\pi^2\rangle \qquad (2)$$

The mixing scenario shows that the wave function of the 2_1^+ state of ^{208}Po should mainly come from neutron excitation. The expected transition strength here is calculated to be $\mathrm{B}_{mix}(E2; 2_1^+ \rightarrow 0_1^+)$ =4.4(4) W.u. which corresponds to $\tau_{theory}(2_1^+)$ =17(2) ps. For better

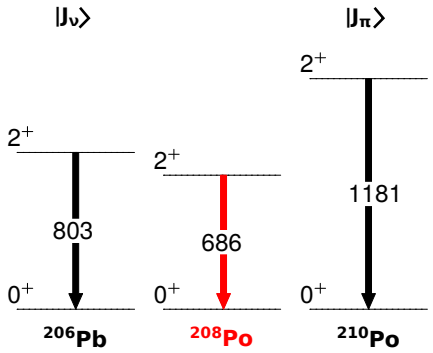

Figure 7. (Color online) The mixing scenario for ^{208}Po. The pure proton and neutron hole excitations of ^{208}Po are assumed to correspond to the excited states of ^{210}Po and ^{206}Pb, respectively.

understanding the structure of ^{208}Po both the precise lifetime of the 2_1^+ state and more thorough theoretical investigations are needed.

Acknowledgements

D.K. acknowledges the support by the Bulgarian Ministry of Education and Science under the National Research Program Young scientists and post-doctoral students approved by DCM No.RD-22-868/08.04.2019 and by the BgNSF under grant KP-06-M28/1 (08/12/2018). This work was supported by the partnership agreement between the University of Cologne and University of Sofia, by the DFG under grants GRH 2128 and SFB 1245, by the BMBF under grants Nos. 05P19RDFN1, 05P18RDCIA. M.S. and P.S. acknowledge financial support by UK-STFC.

References

[1] M.G. Mayer and J.H.D. Jensen, *Elementary Theory of Nuclear Shell Structure* (John Wiley & Sons, Inc., 1955).
[2] R.F. Casten, Phys. Lett. B **152**, 145 (1985).
[3] D. Kocheva *et al.*, Phys. Rev. C **93**, 011303(R) (2016).
[4] D. Kocheva *et al.*, Phys. Rev. C **96**, 044305 (2017).
[5] T.K. Alexander and J.S. Forster, Adv. Nucl. Phys. **10**, 197 (1978).
[6] A. Dewald, O. Möller, and P. Petkov, Prog. Part. Nucl. Phys. **67**, 786 (2012).
[7] M. Stoyanova *et al.*, Journal of Physics: Conference Series, to be publushed.
[8] M. J. Martin, Nucl. Data Sheets **108**, 1583 (2007).
[9] C. Stahl, J. Leske, M. Lettmann, N. Pietralla, Comp. Phys. Com. **214**, (2017) 174.
[10] S. Agostinelli *et al.*, Nucl. Instrum. Methods A **506**, (2003) 250.
[11] L.C. Northcliffe and R.F. Schilling, Nucl. Data Sect. **7**, (1970) 233.
[12] J.F. Ziegler and J.P. Biersack, in *Treatise on Heavy Ion Science*, edited by D.A. Bromley (Plenum Press, New York, 1985), Vol. 6, p. 95.
[13] J.F. Ziegler, M.D. Ziegler and J.P. Biersack, Nucl. Instr Meth., B **268**, (2010) 1823.
[14] J. Keinonen, AIP Conf. Proc. **125**, (1985) 557.
[15] A.Z. Schwarzschild, E.K. Warburton, Ann. Rev. Nucl. Sci. **18**, 265 (1968).
[16] A. Dewald, S. Harissopulos and P. von Brentano, Z. Phys. A **334**, 163 (1989).
[17] G. Böhm, A. Dewald, P. Petkov and P. von Brentano, Nucl. Inst. Meth. A **329**, 248 (1993).